

Low-Temperature Experimental Electron Density Distribution of Formamide

BY E. D. STEVENS

Department of Chemistry, State University of New York at Buffalo, Buffalo, New York 14214, USA

(Received 1 August 1977; accepted 6 September 1977)

The electron density distribution of solid formamide is determined from high-resolution X-ray intensity measurements at 90 K. Bias from the aspherical valence density is reduced by refining only high-order data. H positions and anisotropic thermal parameters are successfully refined from data with $\sin \theta/\lambda > 0.60 \text{ \AA}^{-1}$. Elimination of the bias on O parameters from the lone-pair density requires refinement with $\sin \theta/\lambda > 0.85 \text{ \AA}^{-1}$. Calculation of the estimated error distribution in the experimental densities yields an average error of 0.03 e \AA^{-3} except near atom centers. Peaks in the deformation density are found in all covalent bonds, while no accumulation is found between the N–H donors and O acceptors of the hydrogen bonds. Stereographic projection of the density on a spherical surface about the O atom reveals non-bonded density above and below the molecular plane.

Introduction

The distribution of electron density in a molecule may be obtained directly from accurate X-ray diffraction data (Coppens, 1975; Coppens & Stevens, 1977). Comparison of experimental and theoretical density distributions provides a measure of the reliability of the methods and insight into the deficiencies of both. Since calculation of electron densities of comparable accuracy from theoretical wavefunctions is presently feasible only for small molecules, the number of comparisons between theory and experiment is limited. A quantitative comparison of the theoretical density of the azide ion with the experimental densities in NaN_3 and KN_3 has recently been reported by Stevens, Rys & Coppens (1977a).

The present high-resolution X-ray diffraction study of formamide (Fig. 1) was undertaken to compare the experimental density with a theoretical electron density calculation (Stevens, Rys & Coppens, 1977b). Like N_3^- ,

the formamide molecule is small enough to allow calculation of a near Hartree–Fock wavefunction. The types of bonding features in the formamide molecule are closer to those encountered in biological systems, and the network of hydrogen bonds provides information on the electronic character of hydrogen bonding.

Experimental section

X-ray data collection and reduction

A small drop of Reagent Grade formamide (Fisher Scientific Co.) was sealed in a 0.2 mm glass capillary and centered on a Picker FACS-I diffractometer. The sample was cooled with a stream of cold nitrogen gas generated with a locally modified Enraf–Nonius Universal Low Temperature Device. A single crystal was obtained by slowly translating the cold stream onto the sample at a temperature about 10°C below the melting point ($1\text{--}2^\circ\text{C}$). With patience, the entire sample could be grown into a single crystal (0.20 mm in diameter, 0.50 mm long), as confirmed with oscillation photographs. For data collection, the gas stream was maintained at $90 \pm 5 \text{ K}$ and monitored with a copper–constantan thermocouple.

Crystallographic information is summarized in Table 1. Unit-cell dimensions were obtained by least-squares refinement of the setting angles of 23 centered reflections with $2\theta > 65^\circ$. Intensity measurements were collected with Nb-filtered $\text{Mo K}\alpha$ radiation. The full 2θ step-scan profile of each reflection was recorded on magnetic tape and analyzed to give the integrated intensity and its standard deviation (Blessing, Coppens & Becker, 1974). 2709 reflections were collected in the range $0.0 < \sin \theta/\lambda < 0.80 \text{ \AA}^{-1}$, corresponding to three

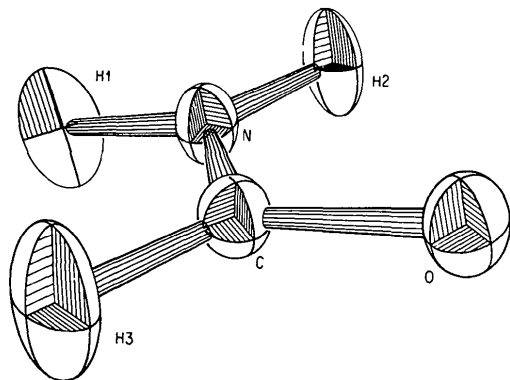


Fig. 1. Formamide 50% probability thermal ellipsoids at 90 K from refinement of high-order X-ray data.

symmetry-related forms of each independent reflection. Three standard reflections measured after every 30 reflections showed long-term fluctuations of $\pm 4\%$ and were used to scale the data by linear interpolation. Absorption corrections were calculated by Gaussian numerical integration. Averaging symmetry-related reflections gave 894 independent reflections.

Since insufficient high-order data were available, a second set of intensity measurements were collected. To reduce the contribution to the error from counting statistics, a larger crystal (0.50 mm in diameter, 0.50 mm long) was used. Since a large proportion of the high-order reflections are weak, parameters from least-squares refinement of the first data set were used to predict the intensities of reflections in the high-order region. Only reflections with intensities predicted to be greater than their estimated standard deviations were measured.* 904 reflections were measured in the range $0.60 < \sin \theta/\lambda < 1.05 \text{ \AA}^{-1}$ corresponding to two symmetry-related forms of each independent reflection. The data were processed in a manner similar to that for the first data set.

Least-squares refinement on reflections in common between the two data sets was used to determine a scale factor relating the two sets. Averaging symmetry-related forms of the merged data sets gave 1125 independent reflections with internal agreement factors of $R(F^2) = 3.3\%$ and $R_w(F^2) = 6.0\%$. For the 216 strongest reflections [$F^2 > 100\sigma(F^2)$] agreement factors were $R(F^2) = 2.0\%$ and $R_w(F^2) = 1.9\%$.

Refinement

The atomic coordinates determined by Ladell & Post (1954) were used as starting parameters for full-matrix least-squares minimization of $\sum w(|F_o| - k|F_c|)^2$ with $w = 1/\sigma^2(F)$. The standard deviation of an observation

* It is expected that such a procedure may bias the results in a similar manner to the exclusion of weak reflections in the refinement (Hirshfeld & Rabinovich, 1973). However, experience has shown that the bias is generally within the estimated standard deviations of the parameters (Griffin & Coppens, 1975).

Table 1. Crystallographic data for formamide at 90 K

Lattice dimensions are from the least-squares refinement based on optimized setting angles of 23 reflections and $\lambda(\text{Mo } K\alpha_1) = 0.70930 \text{ \AA}$.

Space group	$P2_1/n$	V_{cell}	224.68 \AA^3
a	$3.604 (2) \text{ \AA}$	Z	4
b	$9.041 (3)$	$\rho_{\text{X-ray}}$	1.331 g cm^{-3}
c	$6.994 (2)$	μ^*	1.093 cm^{-1}
β	$100.50 (5)^\circ$	M_r	45.04

* Based on mass absorption coefficients from *International Tables for X-ray Crystallography* (1974).

$\sigma(F^2)$ was taken as the larger of σ_1 and σ_2 , where $\sigma_1^2 = \sigma_{\text{counting}}^2 + (0.03F_o^2)^2$ and $\sigma_2^2 = \Sigma^N (F_o^2 - \langle F_o^2 \rangle)^2 / (N-1)$ for N symmetry-related measurements of the reflection. Reflections with both F_o and $F_c < 3\sigma(F_o)$ were considered 'unobserved' and not included in the refinement. Atomic scattering factors were taken from Doyle & Turner (1968) for C, N, and O and from Stewart, Davidson & Simpson (1965) for H. Anomalous scattering factors (C,N,O) were taken from Cromer & Liberman (1970). Positional and anisotropic thermal parameters were refined for all atoms along with the overall scale factor k . Refinement of secondary extinction was found to be unnecessary.

To reduce bias in refined parameters from the aspherical valence electron density distribution, high-order refinements were made using only reflections with $\sin \theta/\lambda > 0.85 \text{ \AA}^{-1}$. High-order parameters for H were obtained in a separate refinement using data with

Table 2. Agreement indices of least-squares refinement

Refinement	I	II	III
$\sin \theta/\lambda$ range (\AA^{-1})	0.0–1.05	0.6–1.05	0.85–1.05
N_{obs}	914	650	119
N_v	55	55	28
Scale factor	7.77 (2)	7.41 (2)	7.51 (29)
R factors			
R	0.040	0.085	0.057
R_w	0.034	0.044	0.038
R factors including rejected reflections			
R	0.067	0.119	0.074
R_w	0.034	0.045	0.039
Goodness of fit	3.105	2.409	1.977

Table 3. Atomic fractional coordinates

Refinement I ($0.00 < \sin \theta/\lambda < 1.05 \text{ \AA}^{-1}$)			
	x	y	z
O	0.4718 (2)	−0.0687 (1)	0.2486 (8)
N	0.2996 (2)	0.1566 (1)	0.1190 (1)
C	0.3358 (2)	0.0565 (1)	0.2580 (1)
H(1)	0.211 (4)	0.244 (1)	0.140 (2)
H(2)	0.367 (4)	0.135 (1)	0.006 (2)
H(3)	0.242 (4)	0.089 (1)	0.378 (1)
Refinement II ($0.60 < \sin \theta/\lambda < 1.05 \text{ \AA}^{-1}$)			
	x	y	z
O	0.4722 (2)	−0.0688 (1)	0.2483 (1)
N	0.2983 (2)	0.1569 (1)	0.1182 (1)
C	0.3351 (2)	0.0565 (1)	0.2581 (1)
H(1)	0.192 (12)	0.256 (4)	0.143 (5)
H(2)	0.383 (12)	0.131 (3)	−0.007 (5)
H(3)	0.246 (18)	0.090 (4)	0.392 (6)
Refinement III ($0.85 < \sin \theta/\lambda < 1.05 \text{ \AA}^{-1}$)			
	x	y	z
O	0.4718 (8)	−0.0684 (2)	0.2485 (3)
N	0.2981 (9)	0.1570 (2)	0.1181 (3)
C	0.3350 (11)	0.0564 (2)	0.2581 (3)
H(1)	Same as II, not refined		
H(2)			
H(3)			

Table 4. Atomic thermal parameters (\AA^2)

	U_{11}	U_{22}	U_{33}	U_{12}	U_{13}	U_{23}
Refinement I						
O	0.0316 (3)	0.0156 (2)	0.0218 (2)	0.0023 (2)	0.0103 (2)	0.0027 (2)
N	0.0295 (4)	0.0149 (2)	0.0205 (3)	0.0030 (3)	0.0094 (3)	0.0003 (2)
C	0.0204 (3)	0.0176 (3)	0.0171 (3)	-0.0010 (3)	0.0051 (3)	0.0015 (2)
H(1)	0.072 (11)	0.050 (9)	0.018 (6)	0.009 (8)	0.027 (7)	0.024 (6)
H(2)	0.063 (10)	0.009 (6)	0.051 (8)	0.018 (6)	0.008 (8)	0.009 (6)
H(3)	0.043 (9)	0.015 (5)	0.018 (5)	0.005 (5)	0.017 (6)	-0.001 (5)
Refinement II						
O	0.0253 (3)	0.0149 (2)	0.0209 (2)	0.0027 (2)	0.0080 (2)	0.0034 (1)
N	0.0248 (3)	0.0147 (2)	0.0195 (2)	0.0029 (2)	0.0077 (2)	0.0006 (1)
C	0.0223 (3)	0.0157 (2)	0.0160 (2)	0.0007 (2)	0.0059 (2)	-0.0002 (2)
H(1)	0.043 (15)	0.028 (11)	0.018 (8)	0.023 (13)	0.001 (8)	0.013 (8)
H(2)	0.047 (17)	0.025 (12)	0.015 (9)	0.010 (10)	0.014 (10)	0.000 (7)
H(3)	0.075 (30)	0.029 (15)	0.020 (12)	0.006 (15)	0.021 (16)	0.000 (9)
Refinement III						
O	0.0254 (24)	0.0154 (6)	0.0192 (7)	0.0028 (7)	0.0081 (7)	0.0033 (6)
N	0.0246 (16)	0.0147 (7)	0.0193 (8)	0.0030 (7)	0.0075 (8)	0.0010 (4)
C	0.0222 (20)	0.0157 (8)	0.0158 (8)	0.0012 (9)	0.0060 (8)	-0.0001 (4)
H(1) } H(2) } H(3) }	Same as II, not refined					

$\sin \theta/\lambda > 0.60 \text{ \AA}^{-1}$. The results of the various refinements are listed in Tables 2, 3 and 4.*

Electron density maps

The effect of chemical bonding on the molecular electron density distribution is conveniently displayed in the deformation density

$$\begin{aligned} \Delta\rho_{\text{deformation}} &= \rho_o/k - \rho_{\text{spherical atom}} \\ &= \frac{1}{V} \sum_{hkl} (F_o/k - F_{\text{spherical atom}}) \exp[-2\pi i(hx + ky + lz)] \end{aligned}$$

where $F_{\text{spherical atom}}$ is calculated from a superposition of isolated spherical Hartree-Fock atom densities and requires positional and thermal parameters free from bias due to the valence electron distribution. The $\Delta\rho_{\text{deformation}}$ corresponds to the change in the 'promolecule' (an assembly of spherical atoms at the atomic positions) upon molecule formation, and is a sensitive function of the details of the electron distribution such as the build-up of density in the bonding and lone-pair regions.

All maps have been calculated using the full X-ray data set, and a scale factor was determined by a cycle of refinement on all the data with fixed high-order parameters.

* A list of structure factors has been deposited with the British Library Lending Division as Supplementary Publication No. SUP 33012 (7 pp.). Copies may be obtained through The Executive Secretary, International Union of Crystallography, 13 White Friars, Chester CH1 1NZ, England.

In addition to the conventional contour plots of planar sections, the electron density distribution calculated for the surface of a sphere has been plotted in stereographic projection. Stereographic projections of the density around the O atom provide a better three-dimensional description of the lone-pair density and its relationship with the hydrogen bonds, than would be possible without plotting a large number of planar sections. Calculation of the density in stereographic projection is described by Stevens & Coppens (1977).

Error maps

To judge the significance of features in the experimental density, it is necessary to estimate the distribution of errors in the deformation density. Considering the contributions from errors in the X-ray intensity measurements, in the refined parameters, and in the X-ray scale factor, the error distribution is given (Rees, 1976) by

$$\sigma(\Delta\rho) = [\sigma^2(\rho_o) + \sigma^2(\rho_c) + \sigma^2(k)\rho_o^2/k^2]^{1/2}$$

assuming the contributions to be uncorrelated. While the first contribution is relatively constant throughout the crystal (except near crystallographic symmetry elements), the second and third contributions peak near the atomic centers, and features of $\Delta\rho$ within about 0.3 \AA of the nuclear positions are often not significant. In calculating $\sigma(\Delta\rho)$, correlations between the positional parameters, thermal parameters, and scale factor from the least-squares refinement have been included. Contributions from $\sigma(\rho_c)$ and $\sigma(k)$ have been calculated analytically (Stevens & Coppens, 1976) and series terminated to the same extent as the experiment.

Results and discussion

Refinement results

Parameters obtained for H from the conventional least-squares refinement of X-ray data clearly show the bias introduced by the bonding density. In formamide, the CH and NH distances are ~ 0.1 Å shorter than expected from neutron diffraction studies (in which the nuclear positions rather than the centroid of charge are measured) on other compounds. Heavier atoms show similar shifts. For the O atom, refinement with data above 0.60 Å⁻¹ in $\sin \theta/\lambda$ shifts the O position toward the lone pairs which are sharper features and therefore scatter to higher angles than the C=O bonding density. The O position does not converge until the minimum value of $\sin \theta/\lambda$ used in the refinement is increased to 0.85 Å⁻¹. Also, as the temperature is lowered and thermal motion decreases, the valence features will scatter to higher angles. Therefore, the optimum low-angle cut-off for the data in a high-order refinement will depend on the type of atoms present and on the temperature.

Since H has no core electrons, there is little contribution to the scattering at high angles and therefore it is difficult to obtain unbiased parameters from a high-order refinement of the X-ray data. With high-accuracy data, however, there appears to be a small cusp of density around the nucleus which contributes to scattering at high angles. A few other studies have been reported in which H parameters have been successfully refined with isotropic thermal parameters from high-order data (Ottersen & Hope, 1976; Iwata & Saito, 1973).

Since there is no reason to expect the thermal motion in the formamide structure to be isotropic, anisotropic thermal parameters have been refined for H atoms. Although the statistical accuracy of the H parameters obtained from high-order refinement is low, the values are in reasonable agreement with the results from other techniques (Table 5), and the probability ellipsoids are in reasonable agreement with a rigid-body-motion model for the molecule. If a Hartree-Fock scattering factor is used for the H, the temperature factors become non-positive definite.

Bond distances and angles calculated from full-data and high-angle refinements are compared with gas-phase electron diffraction and microwave values in Table 5. The CN and NH bond lengths as found in the high-order refinement are in good agreement with the corresponding gas-phase values. The CO bond distance is significantly longer and the CN bond shorter in the crystal, the effect of hydrogen bonding apparently decreasing and increasing the double-bond character of the CO and CN bonds respectively. Similar differences are found for other small amides and acids (Kitano & Kuchitsu, 1974). The lengthening of the CO bond is

Table 5. Bond distances and angles

	X-ray Full data	X-ray High order*	Electron diffraction ^a	Microwave ^b
Bond distances (Å)				
C=O	1.241 (1)	1.239 (4)	1.211 (4)	1.219 (12)
C-N	1.318 (1)	1.326 (4)	1.367 (4)	1.352 (12)
C-H(3)	1.01 (1)	1.09 (5)	1.12 ^c	1.098 (10)
N-H(1)	0.87 (1)	1.01 (5)	1.021 (9) ^d	1.002 (3)
N-H(2)	0.89 (1)	1.01 (5)	1.021 ^d	1.002 (3)
Bond angles (°)				
N-C=O	125.0 (1)	124.9 (3)	124.9 (5)	124.7 (3)
N-C-H(3)	114.5 (6)	116 (3)	112.7 ^c	112.7 (2)
C-N-H(1)	118.9 (7)	118 (3)	120.0 ^c	120.0 (3)
C-N-H(2)	119.6 (7)	119 (3)	118.5 ^c	118.5 (5)

(a) Kitano & Kuchitsu (1974). (b) Hirota, Sugisaki, Nielsen & Sørensen (1974). (c) Fixed. (d) Constrained $r_{N-H(1)} = r_{N-H(2)}$.

* $(\sin \theta/\lambda)_{\min} = 0.85$ Å⁻¹ for O, N, C parameters; 0.60 Å⁻¹ for H parameters.

somewhat larger than found for barbiturates (Craven, Cusatis, Gartland & Vizzini, 1973).

In the crystal, formamide molecules are linked by two types of hydrogen bonds as described by Ladell & Post (1954). A N-H(2)···O' hydrogen bond [2.948 (3) Å] joins the molecules in dimers about a center of symmetry and a N-H(1)···O'' hydrogen bond [2.885 (3) Å] joins alternate dimers into chains. The refined H positions of the present study give H(2) to O' and H(1) to O'' distances of 1.94 (5) and 1.90 (6) Å respectively, making the two types of interactions essentially equal. The molecule is planar within the estimated standard deviations of all of the atom positions. The equation of the weighted least-squares plane is $3.0769x + 3.2532y + 1.5255z = 1.6080$.

Translational and librational tensors obtained from a rigid-body fit to the individual thermal parameters (Schomaker & Trueblood, 1968) are listed in Table 6. Refinement of a screw tensor did not significantly improve the fit.

Table 6. Results of rigid-body thermal motion analysis (L and T relative to inertial axes)

L (rad ²)	0.0261 (26)	-0.0046 (16)	-0.0029 (17)
		0.0067 (16)	-0.0012 (12)
			0.0037 (11)
T (Å ²)	0.0157 (19)	0.0007 (18)	-0.0023 (21)
		0.0118 (23)	0.0006 (24)
			0.0177 (34)

Transformation from crystal axes to inertial axes of unit length

0.7074	-8.0859	2.5273
1.7081	-2.4828	-6.3617
3.1003	3.2129	1.4444

Radial dependence and net atomic charge

Any attempt to divide the electron density distribution of a crystal among atoms to yield atomic charges will be, to some extent, arbitrary. However, the concept of net atomic charges in a molecule has been found to be a chemically useful concept and gives an approximate description of the overall charge distribution.

Approximate net charges may be obtained from the experimental measurements by least-squares refinement of the occupancy of the valence density functions. Consistent results are obtained when the radial dependence of the valence density is also adjusted by refinement of an additional parameter κ for each atom such that

$$\rho'(r) = \rho_{\text{valence}}(\kappa r) + \rho_{\text{core}}(r).$$

A value of κ greater or less than 1.0 corresponds to a contraction or expansion of the atomic density relative to the reference state (Yang, Becker & Coppens, 1977).

The results of a refinement of the atomic charges and radial dependence of the atoms in the structure of formamide are compared with a population analysis of the theoretical wavefunction of Christensen, Kortzborn, Bak & Led (1970) in Table 7. As expected, atoms with net negative charges are expanded relative to Hartree-Fock atoms and those with positive charges are contracted. The H atoms are highly contracted relative to the isolated atom as predicted from theory and experimental experience (Stewart, Davidson & Simpson, 1965). If the molecule is not constrained to be neutral, all atomic charges become more negative by about 0.08 e in the refinement.

Electron density maps

The deformation density calculated in the plane of the formamide molecule is shown in Fig. 2. Peaks are found between atoms corresponding to covalent bonding and in the lone-pair region of the O atom. The distribution of errors in the same plane is also plotted in Fig. 2. The estimated $\sigma(\Delta\rho)$ is $0.03 \text{ e } \text{Å}^{-3}$ except near the atomic centers. The estimated error increases to 0.15, 0.13, and $0.12 \text{ e } \text{Å}^{-3}$ at the O, N, and C

Table 7. Net atomic charge and valence radial dependence

	Experimental		Theoretical charge*
	κ	Charge	
O	0.966 (6)	-0.55 (4)	-0.479
N	0.968 (7)	-0.78 (7)	-0.584
C	1.059 (12)	0.51 (8)	0.498
H(1)	1.43 (5)	0.39 (3)	0.280
H(2)	1.43 (5)	0.40 (3)	0.300
H(3)	1.31 (4)	0.03 (3)	-0.015

* Christensen *et al.* (1970).

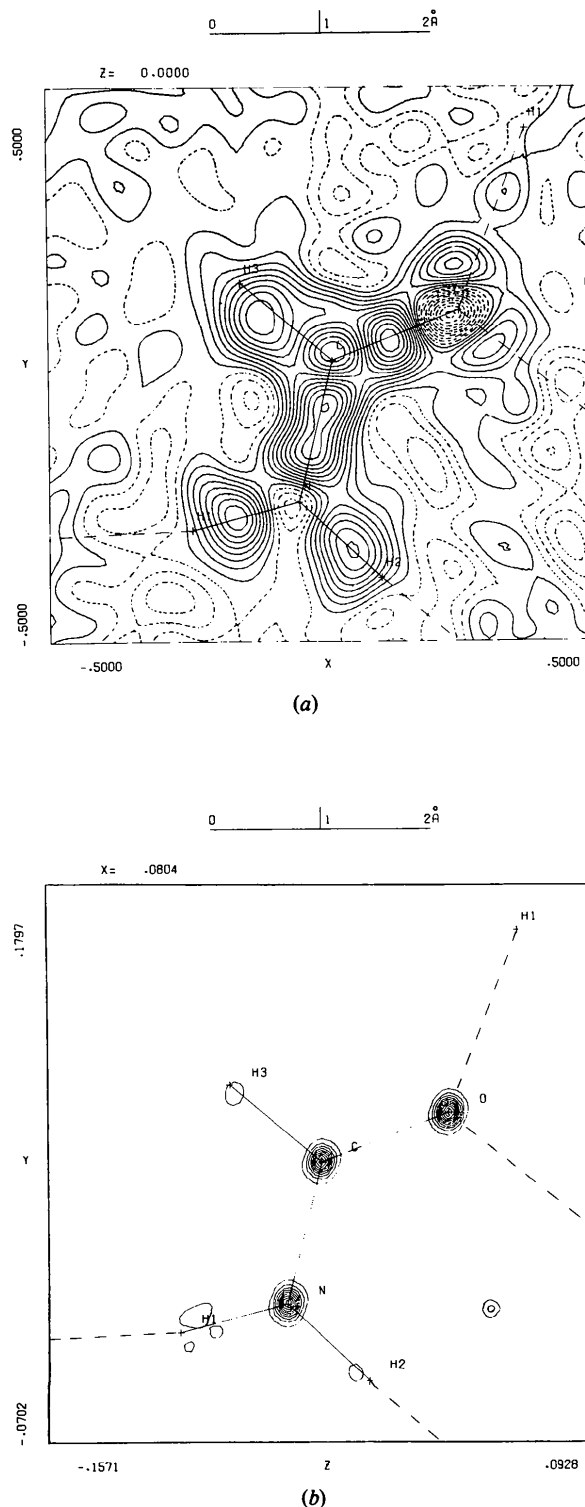


Fig. 2. (a) Experimental deformation density in the least-squares plane of the formamide molecule. Contours are at $0.05 \text{ e } \text{Å}^{-3}$ with negative contours dashed. (b) Estimated error distribution of the deformation density in the molecular plane. Contours at $0.01 \text{ e } \text{Å}^{-3}$, lowest contour plotted at $0.04 \text{ e } \text{Å}^{-3}$.

positions. Despite the large uncertainties associated with the H parameters, the errors near the H atoms are relatively small owing to the much smaller density at the atoms.

In Fig. 3, the average bond and lone-pair peak heights are plotted as a function of the upper limit of data included. As the resolution of the map is increased, more details of the bonding features are included but also more noise from the lower statistical accuracy of the high-order reflections. The behavior of a particular feature will depend both on its curvature and the amount of thermal motion (Coppens & Lehmann, 1976). It is common practice to choose an upper limit in calculating maps as a compromise between neglecting information and increasing noise in the maps (Wang, Blessing, Ross & Coppens, 1976). A plot as in Fig. 3 allows one to determine if particular features have converged to their limit at infinite resolution. For example, the peaks in the bonding region do not increase above a limit of $\sin \theta/\lambda = 0.75 \text{ \AA}^{-1}$. On the other hand, the lone-pair peaks continue to increase out to 0.95 \AA^{-1} .

The C—N bond peak of the deformation density is elongated along the bond axis. The elongated shape appears only if high-order reflections are included in calculating the density. Similar peak shapes have been found in other high-resolution studies, *i.e.* KN_3 (Stevens, 1977), and the low-temperature studies of sodium hydrogen diacetate (Stevens, Lehmann & Coppens, 1977), and glycylglycine (Kvick, Koetzle & Stevens, 1977). The shape results in a peak height at the bond midpoint which first increases and then decreases with increasing high-order limit. The low-order terms in the Fourier series apparently overestimate the peak height while the higher-order terms decrease the density at the center and increase it at the ends of the bond.

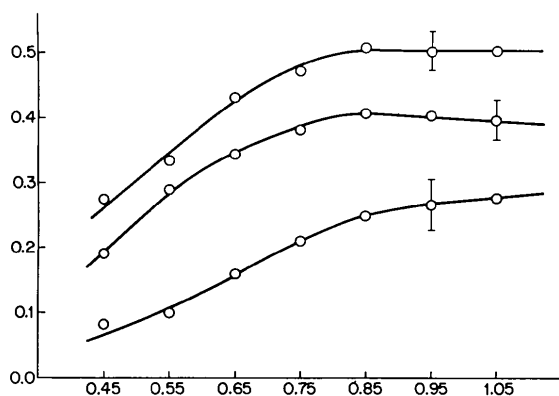


Fig. 3. Average bond and lone-pair peak heights plotted as a function of $(\sin \theta/\lambda)_{\max}$. Upper curve is average of CH and NH bond peaks; middle curve, CN and CO bond peaks; and lower curve the lone-pair peaks.

The density in the hydrogen bonds is shown in Fig. 4. As in previous studies on glycine (Almlöf, Kvick & Thomas, 1973), glycylglycine (Griffin & Coppens, 1975), and 2-amino-5-chloropyridine (Kvick, Thomas & Koetzle, 1976), no density is found between the donor and the acceptor of the hydrogen bond. This is consistent with an interaction for hydrogen bonding which is primarily electrostatic. Theoretical calculations of the difference between dimer density and the sum of monomer densities show a similar slight charge depletion in the hydrogen bond (Dreyfus & Pullman, 1970; Kollman & Allen, 1970; Yamabe & Morokuma, 1975). In contrast, in the short symmetrical hydrogen bond of sodium hydrogen diacetate a build up of charge is found indicating substantial covalent character (Stevens, Lehmann & Coppens, 1977).

Stereographic projections of the deformation density on a sphere of 0.395 \AA radius around the O atom are plotted in Fig. 5. Although two peaks of 0.23 and 0.31 e \AA^{-3} are found in the experimental density plotted in the molecular plane (Fig. 2) as expected for sp^2 hybridization of the O atom, the density projections indicate that the true maxima lie above and below the molecular plane. A similar orientation of the non-bonded density peaks perpendicular to the molecular plane has been observed for the O atom of acetamide in the allenedicarboxylic acid-acetamide complex (Berkovitch-Yellin, 1976). However, the corresponding O atom of the allenedicarboxylic acid bears lone-pair

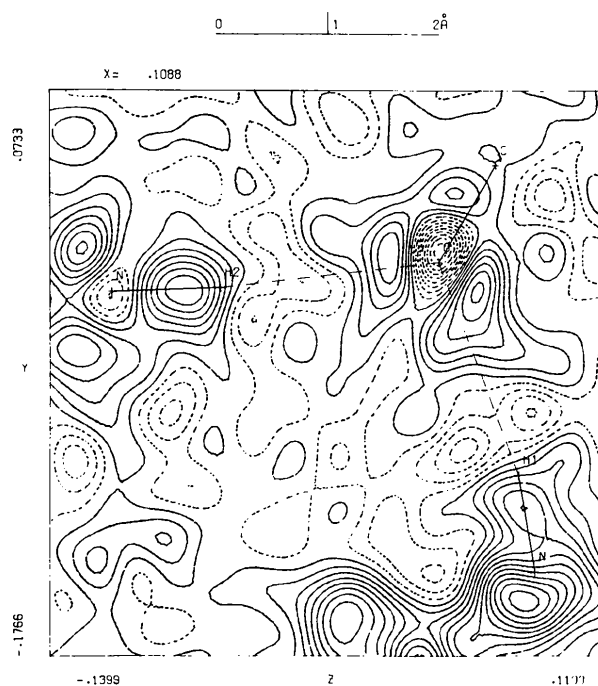


Fig. 4. Hydrogen-bond deformation density in the plane defined by H(1), H(2), and O. Contours as in Fig. 2(a).

peaks in the plane, as is commonly found for other molecules containing carboxylic acid groups (Coppens, Sabine, Delaplane & Ibers, 1969; Stevens, Lehmann & Coppens, 1977).

Since the orientation of non-bonded density is not predicted by theoretical calculation of the isolated

molecule (Stevens, Rys & Coppens, 1977b), it is likely related to the change on forming hydrogen bonds in the solid. The large change in bond lengths (+0.03 and -0.04 Å for the C=O and C-N bonds) in going from the gas phase to the solid indicates a substantial change in electronic structure. Sections of the deformation

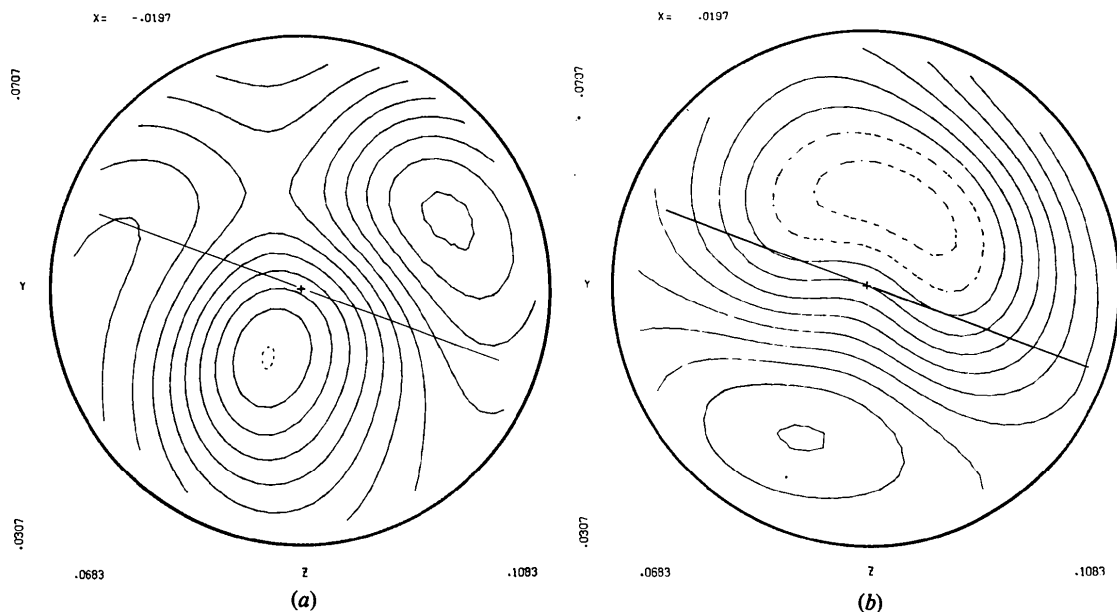


Fig. 5. Stereographic projection of the deformation density at 0.395 Å from the O atom onto a plane perpendicular to the CO bond. Contours as in Fig. 2(a). (a) Projection of the hemisphere opposite the CO bond. (b) Projection of the hemisphere on the side of the CO bond. The orientation of the molecular plane is indicated by a straight line.

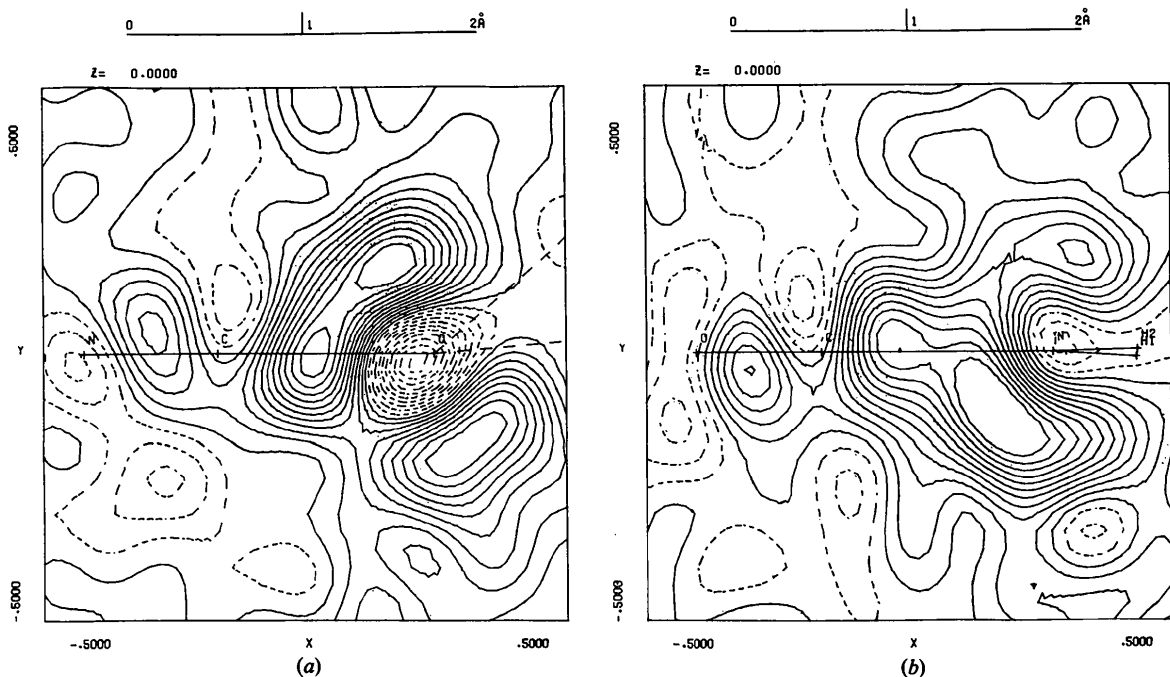


Fig. 6. Sections of the deformation density perpendicular to the molecular plane, (a) through the CO bond, and (b) through the CN bond. Contours as in Fig. 2(a).

density perpendicular to the molecular plane and containing the C=O and C-N bonds are plotted in Fig. 6. Both bond peaks extend well above and below the molecular plane and are polarized toward the electro-negative atom.

In many studies, lone-pair density is found in the same direction in which the O atom accepts hydrogen bonds. This might indicate a directional influence of the lone-pair density on hydrogen bonding. In formamide, however, the non-bonded density about O does not coincide with the hydrogen-bond directions. Calculations of the electrostatic potential in α -glycine (Almlöf, Kvick & Thomas, 1973) show little variation in the potential as a function of the lone-pair directions. If the hydrogen-bonding interaction is primarily electrostatic, the configuration found for formamide would not be significantly unfavorable.

Support of this work by the National Science Foundation is gratefully acknowledged. The author is indebted to Dr P. Coppens for many helpful discussions.

References

- ALMLÖF, J., KVICK, Å. & THOMAS, J. O. (1973). *J. Chem. Phys.* **59**, 3901–3906.
- BERKOVITCH-YELLIN, Z. (1976). PhD Thesis, Weizmann Institute of Science, Israel.
- BLESSING, R. H., COPPENS, P. & BECKER, P. (1974). *J. Appl. Cryst.* **7**, 488–492.
- CHRISTENSEN, D. H., KORTZEBORN, R. N., BAK, B. & LED, J. J. (1970). *J. Chem. Phys.* **53**, 3912–3922.
- COPPENS, P. (1975). *MTP International Review of Science: Physical Chemistry*. Ser. 2, Vol. 11. London: Butterworths.
- COPPENS, P. & LEHMANN, M. S. (1976). *Acta Cryst.* **B32**, 1777–1784.
- COPPENS, P., SABINE, T. M., DELAPLANE, R. G. & IBERS, J. A. (1969). *Acta Cryst.* **B25**, 2451–2458.
- COPPENS, P. & STEVENS, E. D. (1977). *Adv. Quantum Chem.* **10**, 1–35.
- CRAVEN, B. M., CUSATIS, C., GARTLAND, G. L. & VIZZINI, E. A. (1973). *J. Mol. Struct.* **16**, 331–342.
- CROMER, D. T. & LIBERMAN, D. (1970). *J. Chem. Phys.* **53**, 1891–1898.
- DOYLE, P. A. & TURNER, P. S. (1968). *Acta Cryst.* **A24**, 390–397.
- DREYFUS, M. & PULLMAN, A. (1970). *Theor. Chim. Acta*, **19**, 20–37.
- GRIFFIN, J. F. & COPPENS, P. (1975). *J. Am. Chem. Soc.* **97**, 3496–3505.
- HIROTA, E., SUGISAKI, R., NIELSEN, C. J. & SØRENSEN, G. O. (1974). *J. Mol. Spectrosc.* **49**, 251–267.
- HIRSHFELD, F. L. & RABINOVICH, D. (1973). *Acta Cryst.* **A29**, 510–513.
- International Tables for X-ray Crystallography* (1974). Vol. IV, p. 61. Birmingham: Kynoch Press.
- IWATA, M. & SAITO, Y. (1973). *Acta Cryst.* **B29**, 822–832.
- KITANO, M. & KUCHITSU, K. (1974). *Bull. Chem. Soc. Jpn.* **47**, 67–72.
- KOLLMAN, P. A. & ALLEN, L. C. (1970). *J. Chem. Phys.* **52**, 5085–5094.
- KVICK, Å., KOETZLE, T. F. & STEVENS, E. D. (1977). To be published.
- KVICK, Å., THOMAS, R. & KOETZLE, T. F. (1976). *Acta Cryst.* **B32**, 224–231.
- LADELL, J. & POST, B. (1954). *Acta Cryst.* **7**, 559–564.
- OTTERSEN, T. & HOPE, H. (1976). *Am. Crystallogr. Assoc. Abstr. Ser.* **2**, **4**, 54.
- REES, B. (1976). *Acta Cryst.* **A32**, 483–488.
- SCHOMAKER, V. & TRUEBLOOD, K. N. (1968). *Acta Cryst.* **B24**, 63–76.
- STEVENS, E. D. (1977). *Acta Cryst.* **A33**, 580–584.
- STEVENS, E. D. & COPPENS, P. (1976). *Acta Cryst.* **A32**, 915–917.
- STEVENS, E. D. & COPPENS, P. (1977). *J. Cryst. Mol. Struct.* In the press.
- STEVENS, E. D., LEHMANN, M. S. & COPPENS, P. (1977). *J. Am. Chem. Soc.* **99**, 2829–2831.
- STEVENS, E. D., RYS, J. & COPPENS, P. (1977a). *J. Am. Chem. Soc.* **99**, 265–267.
- STEVENS, E. D., RYS, J. & COPPENS, P. (1977b). *J. Am. Chem. Soc.* Submitted for publication.
- STEWART, R. F., DAVIDSON, E. R. & SIMPSON, W. T. (1965). *J. Chem. Phys.* **42**, 3175–3187.
- WANG, Y., BLESSING, R. H., ROSS, F. K. & COPPENS, P. (1976). *Acta Cryst.* **B32**, 572–578.
- YAMABE, S. & MOROKUMA, K. (1975). *J. Am. Chem. Soc.* **97**, 4458–4465.
- YANG, Y. W., BECKER, P. & COPPENS, P. (1977). To be published.